solids

Article

Towards Recognition of Scale Effects in a Solid Model of Lattices with Tensegrity-Inspired Microstructure

Wojciech Gilewski * and Anna Al Sabouni-Zawadzka

Faculty of Civil Engineering, Warsaw University of Technology, Al. Armii Ludowej 16, 00-637 Warsaw, Poland; a.sabouni@il.pw.edu.pl
* Correspondence: w.gilewski@il.pw.edu.pl; Tel.: +48-22-234-5753

Abstract: This paper is dedicated to the extended solid (continuum) model of tensegrity structures or lattices. Tensegrity is defined as a pin-joined truss structure with an infinitesimal mechanism stabilized by a set of self-equilibrated normal forces. The proposed model is inspired by the continuum model that matches the first gradient theory of elasticity. The extension leads to the second- or higher-order gradient formulation. General description is supplemented with examples in 2D and 3D spaces. A detailed form of material coefficients related to the first and second deformation gradients is presented. Substitute mechanical properties of the lattice are dependent on the cable-to-strut stiffness ratio and self-stress. Scale effect as well as coupling of the first and second gradient terms are identified. The extended solid model can be used for the evaluation of unusual mechanical properties of tensegrity lattices.

Keywords: tensegrity; lattice; solid model; microstructure; scale effect

Citation: Gilewski, W.; Sabouni-Zawadzka, A.A. Towards Recognition of Scale Effects in a Solid Model of Lattices with Tensegrity-Inspired Microstructure. *Solids* **2021**, *2*, 50–59. https://doi.org/10.3390/solids2010002

Received: 1 December 2020
Accepted: 8 January 2021
Published: 20 January 2021

1. Introduction

Tensegrity structures or lattices [1–3], due to their special and unusual properties, constitute an interesting concept, the use of which is promising on various scales of considerations in aerospace, civil and mechanical engineering, etc. The main advantages of tensegrity include: large stiffness-to-mass ratio, reliability, controllability, and programmable deployment. There are numerous definitions of tensegrity structures. For the purposes of this study, we define tensegrity as a pin-joined truss structure, in which there is an infinitesimal mechanism balanced by a self-equilibrated system of normal forces, usually called self-stress [4]. Description of various tensegrity structures can be found in the literature e.g., [1–3,5,6]. Tensegrity modules or lattices can be considered as smart structures [5]. Inherent properties of tensegrity structures [7,8] are defined as: self-control, self-diagnosis, self-repair, and active control. Tensegrity may have a modular structure, and then the properties of the entire structure correspond to the characteristics of the module. The analysis of two-dimensional modules, along with the precise definition of tensegrity and tensegrity-like structures, is presented in [9]. A wide analysis of three-dimensional modules can be found e.g., in the papers [1,2,10].

An interesting current trend concerns tensegrity-inspired metamaterials. The concept of tensegrity metamaterials was introduced in [11] and developed in [12–14], where the dynamics of a chain of tensegrity prisms was investigated. In [15] optimal problem for a prototypical self-similar tensegrity column was studied. Morphological optimization of tensegrity-based metamaterials was presented in the work [16]. Another paper [17] focused on formulation of novel cells that could be applied in mechanical metamaterials. Innovative metamaterials and lattices were discussed in [18] with the focus on the geometrically nonlinear behavior of tensegrity prisms with extreme properties. Construction of 3D tensegrity lattices using elementary cells based on the truncated octahedron was discussed in [19] and expanded for phase transition in [20]. The authors in [21] proposed automatically assembled lattices aimed at large-scale applications. Another interesting concept was presented in [22,23], where metal rubber was applied in the struts of a tensegrity mechanical metamaterial. In [24], smart properties and negative Poisson's ratio were discussed using an example of an orthotropic metamaterial constructed from simplex units. In conclusion, recent literature shows that tensegrity-based metamaterials and lattices have a great potential, which is reflected in the dynamic development of these systems within the last few years.

Among the tensegrity lattices, the systems that exhibit unusual or extreme mechanical properties are looked for in [25–28]. The ability to control mechanical properties with the self-stress makes the results for lattices with tensegrity-inspired microstructure very promising.

Tensegrity pin-joined truss lattices, planar and spatial, can be relatively easily described by means of a discrete model, using the finite element method [29,30] or directly formulating the task algebraically [31–33]. Both techniques are formally precise and make it possible to include in the description the influence of self-equilibrated normal force systems (self-stress) on the structural response. The finite element formalism (FE) is algorithmically easy and is based on the standard FE steps from the separate element analysis, through globalization, to consider boundary conditions. The algebraic direct formulation is mathematically elegant, but requires the formulation of global matrices at the beginning of the process. The equivalence of both techniques was demonstrated in [33].

The general characteristics of tensegrity modules and lattices, as well as the identification of substitute mechanical properties can be performed using the continuum model [10,24,34–36]. The idea proposed for the first time in [34] is based on the comparison of the tensegrity strain energy contained in a typical volume determined using a discrete formulation with the strain energy of the solid model, which corresponds to the same volume within the linear theory of elasticity [37]. The description uses the expansion of nodal displacements of the discrete model into Taylor series, limiting further analysis to low-order terms, which in the case of the first approximation leads to the linear theory of elasticity [37] in terms of the theory of the first gradient of deformation. Such a model makes it possible to determine the equivalent mechanical properties in the range of material symmetries acceptable in the linear theory of elasticity [10,38].

The aim of this paper is to generalize the continuum first approximation model [34] to models that take into account higher gradients of displacements. The theories of higher gradients appeared in the literature in the mid-1960s [39,40]. A methodical description of the theory against the background of other possible formulations is presented in [41]. Among numerous papers on the theory of higher gradients, the following papers are worth mentioning: paper [42] in which gradient formulations in relation to simple lattice models are discussed; paper [43] in which an overview of the formulation and length scale identification procedures is given; and paper [44] in which the stress gradient continuum theory is discussed. A solid model in the field of the theory of higher gradients makes it possible to identify the effect of scale, to determine the applicability range of the first approximation theory and to identify problems that should be taken into consideration when dealing with tensegrity structures on a non-micro scale. The present paper describes an extended continuum model and provides a detailed form of material coefficients related to the first and second deformation gradients for selected tensegrity modules or lattices. The lattices are to be consistent with the modules in terms of the infinitesimal mechanism. The examples in 2D and 3D spaces are presented. In the opinion of the authors, the explicit determination of the scale effect and the detailed form of the model coefficients (including their dependence on geometry and self-stress) may constitute a promising contribution to further research on unusual mechanical properties of tensegrity lattices.

The authors' intention is to constitute an attempt towards recognition of scale effects in a solid model of tensegrity-inspired lattices. The proposed technique allows for identification of the strain energy members responsible for the higher gradient theories related to the scale effect factors. Evident identification of scale effects requires validation through a series of tensegrity-based benchmark problems carefully selected for the area of potential applications, e.g., in aerospace engineering or civil/mechanical engineering. This task is beyond the scope of this study.

2. Lattices with Tensegrity-Inspired Microstructure

Structures with tensegrity features can be considered as metamaterials with a microstructure. Regular modular lattices are shown in Figure 1: in the 2D (Figure 1a) and 3D (Figure 1b) spaces. We assume that single unit cells are tensegrities according to the definition presented above.

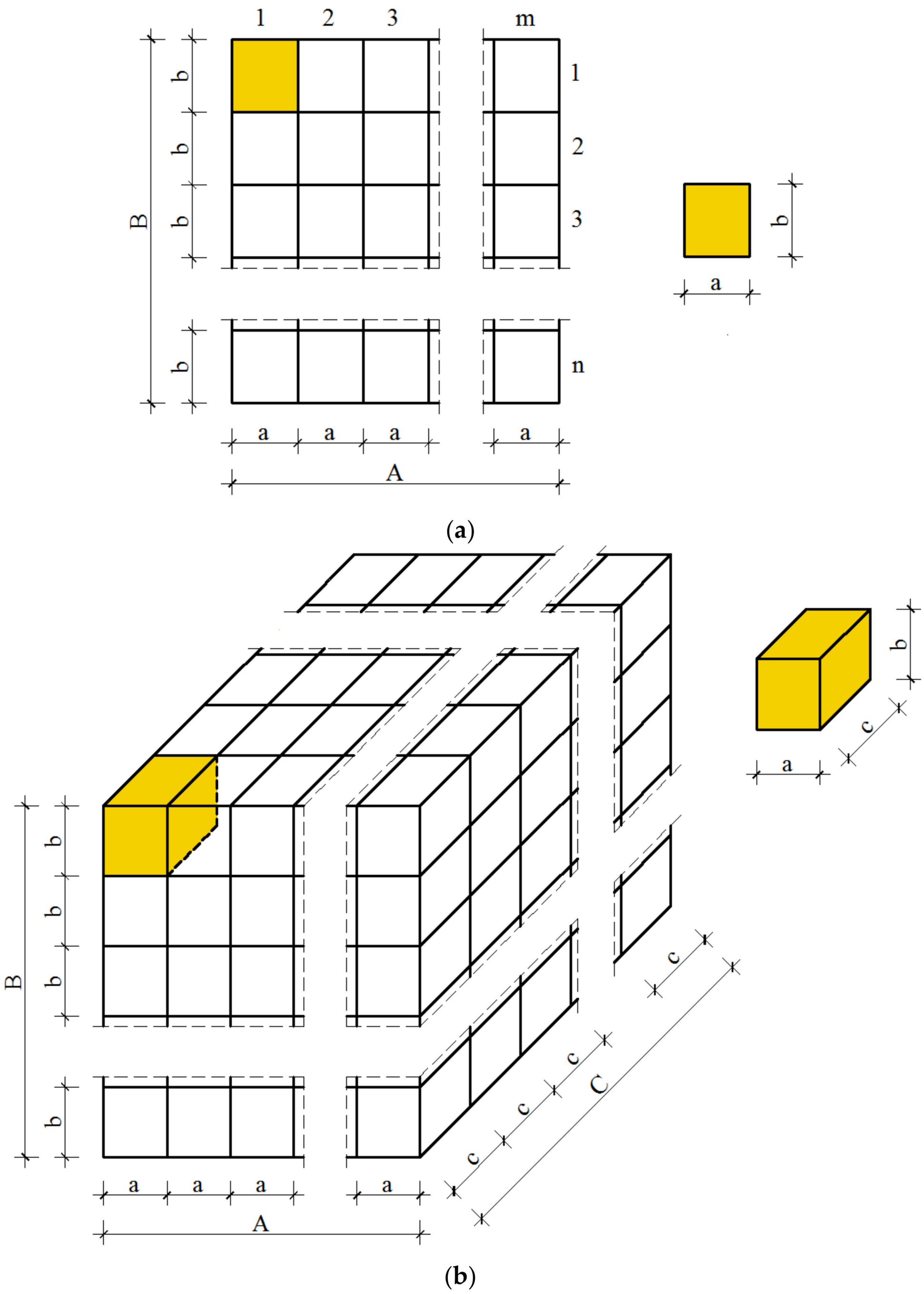

Figure 1. Modular lattices: (**a**) 2D, (**b**) 3D.

As shown in the papers [27,28], the arrangement of lattice modules in a way that ensures the possibility of infinitesimal mechanisms, results in obtaining in the continuum model elasticity matrices with the same material symmetry as can be defined in a single module. This means that it is possible to estimate substitute material properties at the module level. The incompatibility of the infinitesimal mechanisms of the modules in the lattice leads to different material characteristics than in a single module. Then, it is necessary to identify the super-cells in the lattice [27]. In the following part of the paper, we will limit our discussion to lattices with compatible infinitesimal mechanisms.

Figure 2a shows typical regular 2D, hexagonal and tetragonal modules, while Figure 2b shows five typical 3D modules. Modules that do not exhibit self-stress stabilized infinitesimal mechanisms (i.e., they are not tensegrities in the sense of this paper) are not considered, which is quite often found in the available literature. The truth and myths about 2D tensegrity modules are described in [9]. Struts are presented as thick yellow lines and cables are presented as thin black lines.

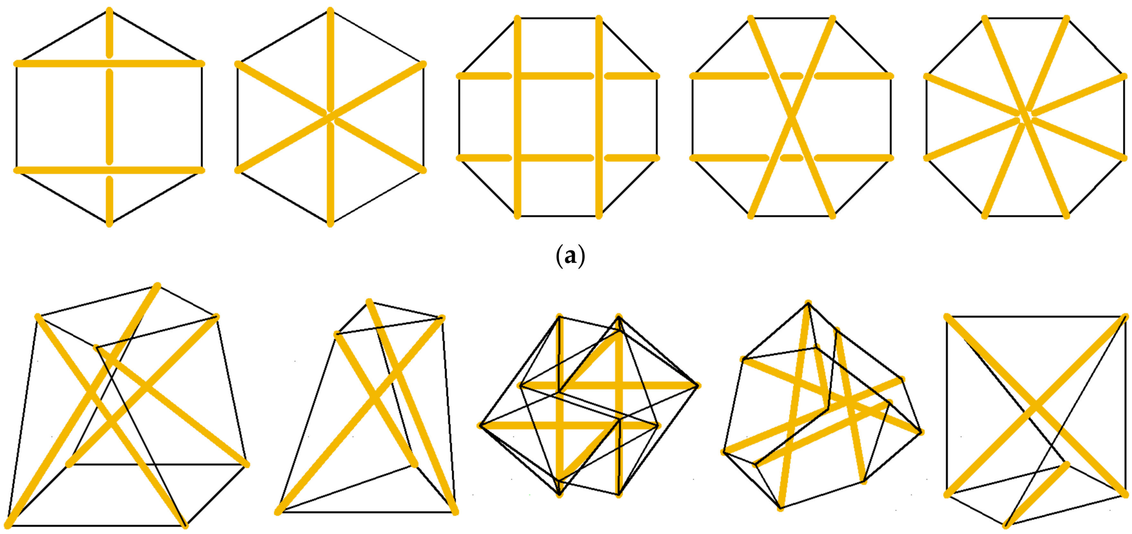

(**a**)

(**b**)

Figure 2. Typical tensegrity modules: (**a**) 2D, (**b**) 3D.

The construction of modular lattices sometimes requires the use of additional cables. Their influence on the material properties of the structure can be usually neglected, but for precision in such cases a repetitive super-cell of the lattice should be specified.

The choice of tensegrity modules for lattices is not limited to that shown in Figures 1 and 2, but is formally unlimited depending on the imagination and needs of the designer.

3. Enhanced Solid Model—Size Effect

Let us consider a lattice tensegrity, with a modular structure compatible with the infinitesimal mechanisms of the modules [27]. Geometry of the lattice is to be defined. Truss theory matrices [29–33] can be obtained with the use of the finite element method [29,30] or algebraically [31–33] without finite element approximation. Distribution of self-equilibrated forces (self-stress) can be found for tensegrity geometry using the singular value decomposition (SVD) of compatibility matrix [32,33]. In a discrete model (DM), the strain energy of a tensegrity truss can be expressed as a quadratic form of nodal displacements $\mathbf{q}$ [29–32]:

$$E_{\mathrm{s}}^{\mathrm{DM}} = \frac{1}{2}\mathbf{q}^{\mathrm{T}}\mathbf{K}\mathbf{q}, \tag{1}$$

where: $\mathbf{K} = \mathbf{K}_{\mathrm{L}} + \mathbf{K}_{\mathrm{G}}$, $\mathbf{K}_{\mathrm{L}}$—global linear stiffness matrix [31,32], $\mathbf{K}_{\mathrm{G}}$—global geometric stiffness matrix. Geometric stiffness matrix is related to the self-stress distribution [33]. Nodal displacements q_i of the lattice can be expressed by mean values $\overline{q}$ and their derivatives related to the geometric center of the cell of the lattice under consideration using the Taylor series expansion

$$q_i = \overline{q} + \frac{\partial \overline{q}}{\partial x}\Delta x + \frac{\partial \overline{q}}{\partial y}\Delta y + \frac{\partial \overline{q}}{\partial z}\Delta z + \\ + \frac{1}{2}\frac{\partial^2 \overline{q}}{\partial x^2}(\Delta x)^2 + \frac{1}{2}\frac{\partial^2 \overline{q}}{\partial y^2}(\Delta y)^2 + \frac{1}{2}\frac{\partial^2 \overline{q}}{\partial z^2}(\Delta z)^2 \frac{\partial^2 \overline{q}}{\partial x \partial y}\Delta x \Delta y + \frac{\partial^2 \overline{q}}{\partial x \partial z}\Delta x \Delta z + \frac{\partial^2 \overline{q}}{\partial y \partial z}\Delta y \Delta z + \ldots, \tag{2}$$

where $\boldsymbol{\Delta}x, \boldsymbol{\Delta}y, \boldsymbol{\Delta}z$ are the distances of the node i from the geometric center of the cell under consideration. In a discrete model, the parameters q_i are linear displacements in the directions of the axis of the coordinate system [31,32]. The coordinates of the nodes of the tensegrity structure can be related to the dimensions of the cell (or the super-cell) a, b, c by parameters $\alpha_{xi}, \alpha_{yi}, \alpha_{zi}$ and written as follows: $\alpha_{xi}a$, $\alpha_{yi}b$, $\alpha_{zi}c$. Then the parameters of the node i can be described by mean values in the center of the volume with appropriate increments: $\Delta x = \alpha_{xi}a$, $\Delta y = \alpha_{yi}b$, $\Delta z = \alpha_{zi}c$. A detailed description and examples of modeling in this regard can be found in the papers [10,24,28,34].

The use of the Taylor series expansion for all nodal displacements of the structure contained in the unit cell of the volume V, allows to express the strain energy density in the form

$$\widetilde{E}_{\mathrm{s}}^{\mathrm{DM}} = \frac{1}{V}[E_{s11}(\Delta \mathbf{u}) + E_{s12}(\Delta \mathbf{u}, \Delta\Delta \mathbf{u}) + E_{s22}(\Delta\Delta \mathbf{u}) + \ldots] \tag{3}$$

The term "11" depends only on the first displacement gradient, the term "22" only on the second displacement gradient, and the term "12" is a mixed term within the theory of elasticity. Calculations can be performed using mathematical software (Mathematica, Maple), which allows to group individual members of the expansion in any way.

The terms of the Equation (3) can be matrix represented as quadratic or bilinear forms

$$E_{s11}(\Delta \mathbf{u}) = \frac{1}{2}(\Delta \mathbf{u})^T \mathbf{E}_{11}(\Delta \mathbf{u}), \tag{4}$$

$$E_{s12}(\Delta \mathbf{u}, \Delta\Delta \mathbf{u}) = (\Delta \mathbf{u})^T \mathbf{E}_{12}(\Delta\Delta \mathbf{u}), \tag{5}$$

$$E_{s22}(\Delta\Delta \mathbf{u}) = \frac{1}{2}(\Delta\Delta \mathbf{u})^T \mathbf{E}_{22}(\Delta\Delta \mathbf{u}). \tag{6}$$

The energy densities of the higher gradient theory can be determined by analogy.

The matrix $\mathbf{E}_{11}$ corresponds to the first approximation within the first gradient theory and is insensitive to scale effects. It was used in the continuum model and successfully applied to pre-evaluate the mechanical properties of tensegrity structures (see i.e., [24,27,28,34]), to determine the dependence of the substitute Young's moduli, Kirchhoff's moduli, Poisson's ratios, and other technical parameters on the self-stress level and on the cable-to-strut ratio for tensegrity modules and lattices [10,28]. The first approximation model is appropriate when the unit cell is very small. The matrices $\mathbf{E}_{12}$, $\mathbf{E}_{22}$ correspond to the second gradient theory and are sensitive to scale effects. They can be used to assess structures, in which the unit cell is relatively large compared to the dimensions of the entire lattice. Matrices $\mathbf{E}_{12}$, $\mathbf{E}_{22}$ describe the influence of strain variability (understood as the first gradient of displacements) within the cell on the mechanical properties of the lattice. Examples of matrices $\mathbf{E}_{11}$, $\mathbf{E}_{12}$, $\mathbf{E}_{22}$ determination for 2D and 3D tensegrity modules are presented below.

3.1. 2D Hexagonal Tensegrity Module

Let us consider a 2D lattice with a thickness of h (thickness of the 2D panel), built from the modules shown in Figure 3, with compressive-tensile stiffness: $(EA)_{cable}$, $(EA)_{strut} = EA$ (E-Young's modulus, A-cross section), and self-equilibrated system of normal forces with the multiplier S—it is a value by which the prestressing forces in all elements are multiplied, used as an indication of the self-stress level.

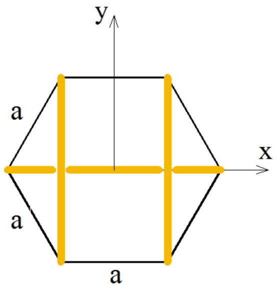

Figure 3. 2D hexagonal tensegrity module.

In the 2D theory of elasticity, the vectors of the first and second displacement gradients have the form

$$\Delta\mathbf{u} = \begin{bmatrix} \frac{\partial u}{\partial x} & \frac{\partial v}{\partial y} & \frac{\partial u}{\partial y} & \frac{\partial v}{\partial x} \end{bmatrix}^T, \tag{7}$$

$$\Delta\Delta\mathbf{u} = \begin{bmatrix} \frac{\partial^2 u}{\partial x^2} & \frac{\partial^2 u}{\partial x \partial y} & \frac{\partial^2 u}{\partial y^2} & \frac{\partial^2 v}{\partial x^2} & \frac{\partial^2 v}{\partial x \partial y} & \frac{\partial^2 v}{\partial y^2} \end{bmatrix}^T \tag{8}$$

Considering only the first gradient theory, the shear strain is usually defined, which is the arithmetic mean of the third and fourth terms of the Equation (7). This leads to smaller dimensions of the elasticity matrix $\mathbf{E}_{11}$, but does not qualitatively change the coefficients of the obtained matrices. The identification of infinitesimal modes and distribution of self-equilibrated normal forces under the considered tensegrity can be found using the singular value decomposition (SVD) of compatibility matrix [31,32,45]. One infinitesimal mode and one set of self-equilibrated normal forces are identified for the 2D module [9]. In the considered example, the following matrices were obtained:

$$\mathbf{E}_{11} = C_1 \frac{\sqrt{3}}{8} \begin{bmatrix} 8+9k & 3k & 0 & 0 \\ 3k & 8+9k & 0 & 0 \\ 0 & 0 & 3k & 0 \\ 0 & 0 & 0 & 3k \end{bmatrix} + C_2 \frac{1}{4} \begin{bmatrix} 1 & -1 & 0 & 0 \\ -1 & 1 & 0 & 0 \\ 0 & 0 & -1 & 0 \\ 0 & 0 & 0 & -1 \end{bmatrix}, \tag{9}$$

$$\mathbf{E}_{12} = 0, \tag{10}$$

$$\mathbf{E}_{22} = a^2 C_1 \begin{bmatrix} 1 & 0 & -1 & 2 & 2 & 0 \\ 0 & 12 & 0 & 0 & 0 & -2 \\ -1 & 0 & 1 & 0 & -2 & 0 \\ 2 & 0 & 0 & 3 & 0 & -3 \\ 2 & 0 & -2 & 0 & 4 & 0 \\ 0 & -2 & 0 & -3 & 0 & 3 \end{bmatrix} + a^2 C_2 \begin{bmatrix} 9 & 0 & -9 & 0 & -6 & 0 \\ 0 & -4 & 0 & -6 & 0 & 6 \\ -9 & 0 & 9 & 0 & 6 & 0 \\ 0 & -6 & 0 & 3 & 0 & -3 \\ -6 & 0 & 6 & 0 & 20 & 0 \\ 0 & 6 & 0 & -3 & 0 & 3 \end{bmatrix}, \tag{11}$$

where: $C_1 = \frac{EA}{ah}$, $C_2 = \frac{S}{ah}$, $k = \frac{(EA)_{cable}}{(EA)_{strut}}$, $(EA)_{strut} = EA$, S is the self-stress multiplier.

In the centro-symmetrical structure of the considered tensegrity the matrix $\mathbf{E}_{12} = 0$, which means that there is no coupling of the first and second displacement gradients in the model. Note that the matrix coefficients depend on the unit cell geometry and the self-stress level. The selection of both these parameters allows, using the matrix $\mathbf{E}_{11}$, to determine possible extreme lattice properties in the form of soft or stiff modes [27,28]. The analysis of the matrix $\mathbf{E}_{22}$ coefficients makes it possible to determine the variability (sensitivity) of individual lattice or unit cell deformation states and to control them to a certain extent using geometric and self-stress parameters. They can be selected so that the second gradient coefficient is as small as possible, or even zero. The scale effect can be observed in the matrix $\mathbf{E}_{22}$ (Equation (11)).

3.2. 3D 4-Strut Simplex Tensegrity Module

Let us consider a 3D lattice built from the modules shown in Figure 4, with compressive-tensile stiffness:$(EA)_{cable}$, $(EA)_{strut} = EA$ (E-Young's modulus, A-cross section), and self-equilibrated system of normal forces with the multiplier S.

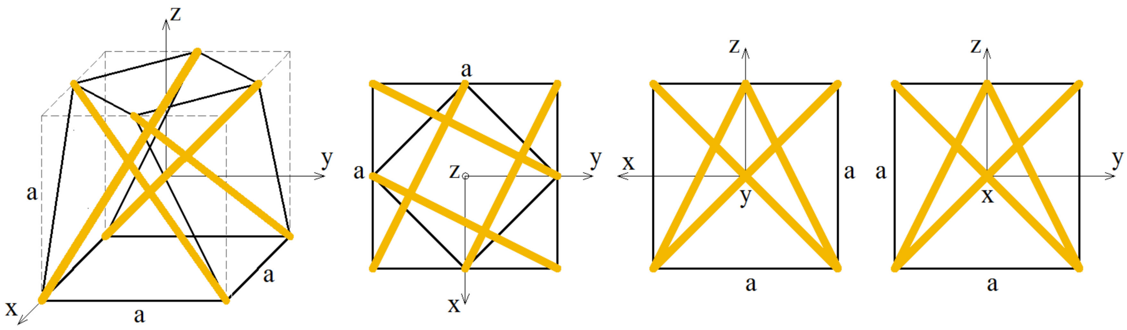

Figure 4. 3D 4-strut Simplex tensegrity module.

In the 3D theory of elasticity, the vectors of the first and second displacement gradients have the form:

$$\Delta\mathbf{u} = \begin{bmatrix} \frac{\partial u}{\partial x} & \frac{\partial v}{\partial y} & \frac{\partial w}{\partial z} & \frac{\partial u}{\partial y} & \frac{\partial v}{\partial x} & \frac{\partial w}{\partial x} & \frac{\partial u}{\partial z} & \frac{\partial v}{\partial z} & \frac{\partial w}{\partial y} \end{bmatrix}^T, \tag{12}$$

$$\Delta\Delta\mathbf{u} = \begin{bmatrix} \frac{\partial^2 u}{\partial x^2} & \frac{\partial^2 u}{\partial y^2} & \frac{\partial^2 u}{\partial z^2} & \frac{\partial^2 u}{\partial x \partial y} & \frac{\partial^2 u}{\partial x \partial z} & \frac{\partial^2 u}{\partial y \partial z} & \frac{\partial^2 v}{\partial x^2} & \frac{\partial^2 v}{\partial y^2} & \frac{\partial^2 v}{\partial z^2} \\ \frac{\partial^2 v}{\partial x \partial y} & \frac{\partial^2 v}{\partial x \partial z} & \frac{\partial^2 v}{\partial y \partial z} & \frac{\partial^2 w}{\partial x^2} & \frac{\partial^2 w}{\partial y^2} & \frac{\partial^2 w}{\partial z^2} & \frac{\partial^2 w}{\partial x \partial y} & \frac{\partial^2 w}{\partial x \partial z} & \frac{\partial^2 w}{\partial y \partial z} \end{bmatrix}^T. \tag{13}$$

As in the example 2D, the identification of infinitesimal modes and distribution of self-equilibrated normal forces in the tensegrity can be found using the SVD decomposition [45]. One infinitesimal mode and one set of self-equilibrated normal forces are identified for the 2D module [10]. In the presented example, due to the large size, we will present the matrices in the following form (with the use of the parameter σ responsible for the self-stress):

$$\mathbf{E}_{11} = \left[E_{11,ij}\right],\ i,j = 1,2,\ldots,9, \tag{14}$$

$$\mathbf{E}_{11} = \begin{bmatrix} E_{11,11} & E_{11,12} & E_{11,13} & E_{11,14} & E_{11,14} & 0 & 0 & 0 & 0 \\ & E_{11,11} & E_{11,13} & -E_{11,14} & -E_{11,14} & 0 & 0 & 0 & 0 \\ & & E_{11,33} & 0 & 0 & 0 & 0 & 0 & 0 \\ & & & E_{11,12} & 0 & 0 & 0 & 0 & 0 \\ & & & & E_{11,12} & 0 & 0 & 0 & 0 \\ & & & & & E_{11,13} & 0 & 0 & 0 \\ & & & & & & E_{11,13} & 0 & 0 \\ & & & & & & & E_{11,13} & 0 \\ sym. & & & & & & & & E_{11,13} \end{bmatrix}$$

$E_{11,11} = E_{11,22} = 2C_0(0.314815 + 1.39827 \cdot k - 0.0794978 \cdot \sigma)$,
$E_{11,12} = E_{11,44} = E_{11,55} = C_0(0.296296 + 0.707107 \cdot k - 0.0134742 \cdot \sigma)$,
$E_{11,13} = E_{11,23} = E_{11,66} = E_{11,77} = E_{11,88} = E_{11,99} = C_0(0.740741 + 0.357771 \cdot k + 0.17247 \cdot \sigma)$,
$E_{11,14} = -E_{11,24} = E_{11,15} = -E_{11,25} = C_0(-0.2222222 - 0.0808452 \cdot \sigma)$,
$E_{11,33} = 2C_0(0.592593 + 1.43108 \cdot k - 0.17247 \cdot \sigma)$.

$$\mathbf{E}_{12} = [E_{12,ik}],\ i = 1,2,\ldots,9, k = 1,2,\ldots,18, \tag{15}$$

$$\mathbf{E}_{22} = [E_{22,kl}],\ i = 1,2,\ldots,1, l = 1,2,\ldots,18, \tag{16}$$

where: $C_0 = \frac{EA}{a^2}$, $k = \frac{(EA)_{cable}}{(EA)_{strut}}$,$(EA)_{strut} = EA$, $\sigma = \frac{S}{EA}$.

Providing the formulas for all coefficients of matrices $\mathbf{E}_{12}$ and $\mathbf{E}_{22}$ exceeds the scope of this study. However, we will give some examples of the coefficients to get an idea of their form:

$$E_{12,71} = aC_0(-0.037037 + 0.894429 \cdot k + 0.0107794 \cdot \sigma),$$
$$E_{12,56} = aC_0(-0.148148 + 0.705105 \cdot k - 0.175105 \cdot \sigma),$$
$$E_{22,11} = a^2C_0(0.00231481 + 0.0497843 \cdot k + 0.00690553 \cdot \sigma),$$
$$E_{22,8-18} = a^2C_0(-0.00538968 + 0.0447214 \cdot k - 0.185185 \cdot \sigma).$$

In the considered 3D tensegrity, due to the lack of center-symmetry of the modules, there is a coupling of the first and second displacement gradients in the model. All three matrices depend on the unit cell geometry and the level of self-stress. The selection of both these parameters allows, using the matrix $\mathbf{E}_{11}$, to determine possible extreme lattice properties in the form of soft or stiff modes [27,28]. The knowledge of the matrix $\mathbf{E}_{11}$ enables the estimation of the equivalent mechanical properties of the module/lattice [10]. Analysis of the matrices $\mathbf{E}_{11}$ and $\mathbf{E}_{22}$ coefficients may allow the assessment of the variability of these properties in different directions of the structure. Scale effects can be observed in the matrices $\mathbf{E}_{12}$ and $\mathbf{E}_{22}$.

4. Conclusions and Future Work

The paper proposes an extended solid model of tensegrity modular lattices (materials or structures with tensegrity-like modular microstructure). The model is based on the discrete model of the structure and expression of nodal displacements by the averaged displacements and their derivatives. Final strain energy depends on the first-, second- and higher-order gradients of displacements.

The main conclusions of the paper can be expressed as:

- Substitute elasticity matrices coefficients depend on the cable to strut stiffness ratio as well as on the self-stress level.
- Coupling of the first and second gradient terms is identified.
- The scale effect can be observed.
- It is possible to determine the variability (sensitivity) of individual lattice or unit cell first gradient deformation states and to control them to a certain extent using geometric and self-stress parameters. They can be selected so that the second gradient coefficient is as small as possible, or even zero.
- The extended solid model can be used for evaluation of unusual mechanical properties of tensegrity lattices.

The proposed technique allows for the identification of the strain energy members responsible for the higher gradient theories related to the scale effect factors. The model is validated for the first-gradient theory in [28]. Evident identification of scale effects requires validation through a series of tensegrity-based benchmark problems carefully selected for the area of potential applications. This is a subject of future work.

Author Contributions: Conceptualization, W.G. and A.A.S.-Z.; methodology, W.G.; software, A.A.S.-Z.; validation, W.G. and A.A.S.-Z.; formal analysis, W.G.; investigation, W.G.; resources, W.G. and A.A.S.-Z.; data curation, W.G. and A.A.S.-Z.; writing—original draft preparation, W.G. and A.A.S.-Z.; writing—review and editing, W.G. and A.A.S.-Z.; visualization, A.A.S.-Z.; supervision, W.G.; project administration, W.G. Both authors have read and agreed to the published version of the manuscript.

Funding: This research received no external funding.

Institutional Review Board Statement: Not applicable.

Informed Consent Statement: Not applicable.

Data Availability Statement: Not applicable.

Conflicts of Interest: The authors declare no conflict of interest.

References

1. Skelton, R.E.; de Oliveira, M.C. *Tensegrity Systems*; Springer: New York, NY, USA, 2009.
2. Motro, R. *Tensegrity: Structural Systems for the Future*; Kogan Page Science: London, UK, 2003.
3. Wroldsen, A.S. Modelling and Control of Tensegrity Structures. Ph.D. Thesis, Department of Marine Technology, Norwegian University of Science and Technology, Trondheim, Norway, 2007; 208p.
4. Calladine, C.R.; Pellegrino, S. First-order infinitesimal mechanisms. *Int. J. Solids Struct.* **1991**, *27*, 505–515. [CrossRef]
5. Gilewski, W.; Al Sabouni-Zawadzka, A. On possible applications of smart structures controlled by self-stress. *Arch. Civ. Mech. Eng.* **2015**, *15*, 469–478. [CrossRef]
6. Adam, B.; Smith, I.F.C. Self-diagnosis and self-repair of an active tensegrity structure. *J. Struct. Eng.* **2007**, *133*, 1752–1761. [CrossRef]

7. Al Sabouni-Zawadzka, A.; Gilewski, W. Inherent smartness of tensegrity structures—Structural elements applications. In Proceedings of the International Association for Shell and Spatial Structures (IASS), Amsterdam, The Netherlands, 17–20 August 2015.
8. Al Sabouni-Zawadzka, A.; Gilewski, W. Inherent smartness of tensegrity structures. *Appl. Sci.* **2018**, *8*, 787. [CrossRef]
9. Obara, P.; Kłosowska, J.; Gilewski, W. Truth and myths about 2D tensegrity trusses. *Appl. Sci.* **2019**, *9*, 179. [CrossRef]
10. Gilewski, W.; Al Sabouni-Zawadzka, A. Equivalent mechanical properties of tensegrity truss structures with self-stress included. *Eur. J. Mech. Solids* **2020**, *83*, 103998. [CrossRef]
11. Fraternali, F.; Carpentieri, G.; Amendola, A.; Skelton, R.E.; Nesterenko, V.F. Multiscale tenability of solitary wave dynamics in tensegrity metamaterials. *Appl. Phys. Lett.* **2014**, *105*, 201903. [CrossRef]
12. Fabbrocino, F.; Carpentieri, G.; Amendola, A.; Penna, R.; Fraternali, F. Accurate numerical methods for studying the nonlinear wave-dynamics of tensegrity metamaterials. *Eccomas Procedia Compdyn* **2017**, 3911–3922. [CrossRef]
13. Amendola, A.; Krushynska, A.; Daraio, C.; Pugno, N.M.; Fraternali, F. Tuning frequency band gaps of tensegrity mass-spring chains with local and global prestress. *Int. J. Solids Struct* **2018**, in press. [CrossRef]
14. Wang, Y.T.; Liu, X.N.; Zhu, R.; Hu, G.K. Wave propagation in tunable lightweight tensegrity metastructure. *Sci. Rep.* **2018**, *8*, 11482. [CrossRef]
15. De Tommasi, D.; Marano, G.C.; Puglisi, G.; Trentadue, F. Optimal complexity and fractal limits of self-similar tensegrities. *Proc. R. Soc. A* **2016**, *471*, 20150250. [CrossRef]
16. De Tommasi, D.; Marano, G.C.; Puglisi, G.; Trentadue, F. Morphological optimization of tensegrity-type metamaterials. *Compos. Part B* **2017**, *115*, 182–187. [CrossRef]
17. Modano, M.; Mascolo, I.; Fraternali, F.; Bieniek, Z. Numerical and analytical approaches to the self-equilibrium problem of class teta = 1 tensegrity metamaterials. *Front. Mech.* **2018**, *5*, 5.
18. Fraternali, F.; Carpentieri, G.; Amendola, A. On the mechanical modeling of the extreme softening/stiffening response of axially loaded tensegrity prisms. *J. Mech. Phys. Solids* **2015**, *74*, 136–157. [CrossRef]
19. Rimoli, J.J.; Pal, R.K. Mechanical response of 3-dimensional tensegrity lattices. *Compos. Part B* **2017**, *115*, 30–42. [CrossRef]
20. Salahsoor, H.; Pal, R.K.; Rimoli, J.J. Material symmetry phase transitions in the three-dimensional tensegrity metamaterial. *J. Mech. Phys. Solids* **2018**, *119*, 382–399. [CrossRef]
21. Zhang, L.Y.; Li, S.X.; Zhu, S.X.; Zhang, B.Y.; Xu, G.K. Automatically assembled large-scale tensegrities by truncated regular polyhedral and prismatic elementary cells. *Compos. Struct.* **2018**, *184*, 30–40. [CrossRef]
22. Zhang, Q.; Zhang, D.; Dobah, Y.; Scarpa, F.; Fraternali, F.; Skelton, R.E. Tensegrity cell mechanical metamaterial with metal rubber. *Appl. Phys. Lett.* **2018**, *113*, 031906. [CrossRef]
23. Ma, Y.; Zhang, Q.; Dobah, J.; Scarpa, F.; Fraternali, F.; Skelton, R.E.; Zhang, D.; Hong, J. Meta-tensegrity: Design of a tensegrity prism with metal rubber. *Compos. Struct.* **2018**, *206*, 644–657. [CrossRef]
24. Al Sabouni-Zawadzka, A.; Gilewski, W. Smart metamaterial based on the simplex tensegrity pattern. *Materials* **2018**, *11*, 673. [CrossRef]
25. Milton, G.; Cherkaev, A.V. Which elasticity tensors are realizable? *J. Eng. Mater. Technol.* **1995**, *117*, 483–493. [CrossRef]
26. Kadic, M.; Buckmann, T.; Stenger, N.; Thiel, M. On the practicability of pentamode mechanical metamaterials. *Appl. Phys. Lett.* **2012**, *100*, 191901. [CrossRef]
27. Al Sabouni-Zawadzka, A. Extreme mechanical properties of regular tensegrity unit cells in 3D lattice metamaterials. *Materials* **2020**, *13*, 4845. [CrossRef] [PubMed]
28. Al Sabouni-Zawadzka, A.; Gilewski, W. Soft and stiff simplex tensegrity lattices as extreme smart metamaterials. *Materials* **2019**, *12*, 187. [CrossRef] [PubMed]
29. Bathe, K.J. *Finite Element Procedures in Engineering Analysis*; Prentice Hall: New York, NY, USA, 1996.
30. Zienkiewicz, O.C.; Taylor, R.L. *The Finite Element Method. Vol. 1. The Basis*; Elsevier Butterworth-Heinemann: London, UK, 2000.
31. Lewiński, T. On algebraic equations of elastic trusses, frames and grillages. *J. Theor. Appl. Mech.* **2001**, *39*, 307–322.
32. Pełczyński, J.; Gilewski, W. Algebraic formulation for moderately thick elastic frames, beams, trusses, and grillages within Timoshenko theory. *Math. Probl. Eng.* **2019**, 7545473. [CrossRef]
33. Pełczyński, J.; Gilewski, W. An extension of algebraic equations of elastic trusses with self-equilibrated system of forces. In Proceedings of the ECCM6, Proceedings of the ECFD7, Glasgow, UK, 11–15 June 2018; R. Owen, R., de Borst, R., Reese, J., Pearce, C., Eds.; CIMNE: Barcelona, Spain, 2018; pp. 4343–4348.
34. Kasprzak, A.; Gilewski, W. 3D continuum model of tensegrity modules with the effect of self0stress. In Proceedings of the WCCM XI, ECCM V, Barcelona, Spain, 20–25 July 2014.
35. Pal, R.K.; Ruzzene, M.; Rimoli, J. A continuum model for nonlinear lattices under large deformations. *Int. J. Solids Struct.* **2016**, *96*, 300–319. [CrossRef]
36. Pal, R.K.; Rimoli, J.; Ruzzene, M. Effect of large deformation pre-loads on the wave properties of hexagonal lattice. *Smart Mat. Struct.* **2016**, *25*, 054010. [CrossRef]
37. Green, A.E.; Zerna, W. *Theoretical Elasticity*; Oxford University Press: Oxford, UK, 1968.
38. Chadwick, P.; Vianello, M.; Cowin, S. A new proof that the number of linear elastic symmetries is eight. *J. Mech. Phys. Solids* **2001**, *49*, 2471–2492. [CrossRef]
39. Mindlin, R.D. Micro-structure in linear elasticity. *Arch. Rat. Mech. Anal.* **1964**, *16*, 51–78. [CrossRef]
40. Mindlin, R.D. Second gradient of strain and surface-tension in linear elasticity. *Int. J. Solids Struct.* **1965**, *1*, 417–438. [CrossRef]

41. Eringen, A.C. *Microcontinuum field theories I: Foundations of Solids*; Springer: New York, NY, USA, 1999.
42. Polyzos, D.; Fotadis, D.I. Derivation of Mindlin's first and sedond strain gradient elastic theory via simple lattice and continuum models. *Int. J. Solids Struct.* **2012**, *49*, 470–480. [CrossRef]
43. Askes, H.; Aifantis, E.C. Gradient elasticity in statics and dynamics: An overview of formulation, length scale identification procedures, finite element implementations and new results. *Int. J. Solids Struct.* **2011**, *48*, 1962–1990. [CrossRef]
44. Forest, S.; Sab, K. Stress gradient continuum theory. *Mech. Res. Comm.* **2012**, *40*, 16–25. [CrossRef]
45. Pellegrino, S. Structural computations with the singular value decomposition of the equilibrium matrix. *Int. J. Solids Struct.* **1993**, *30*, 3029–3035. [CrossRef]